Author for correspondence:

Ivo Siekmann

e-mail:

ivo.siekmann@unimelb.edu.au

Statistical analysis of modal gating in ion channels

Ivo Siekmann [1,2], James Sneyd [3] and Edmund J. Crampin [2,1]

[1] National ICT Australia, Victorian Research Laboratory, Melbourne, Australia
[2] Systems Biology Laboratory, Melbourne School of Engineering, The University of Melbourne, Melbourne, Australia
[3] Department of Mathematics, The University of Auckland, Auckland, New Zealand

Ion channels regulate the concentrations of ions within cells. By stochastically opening and closing its pore, they enable or prevent ions from crossing the cell membrane. However, rather than opening with a constant probability, many ion channels switch between several different levels of activity even if the experimental conditions are unchanged. This phenomenon is known as modal gating: instead of directly adapting its activity, the channel seems to mix sojourns in active and inactive modes in order to exhibit intermediate open probabilities. Evidence is accumulating that modal gating rather than modulation of opening and closing at a faster time scale is the primary regulatory mechanism of ion channels. However, currently, no method is available for reliably calculating sojourns in different modes. In order to address this challenge, we develop a statistical framework for segmenting single-channel data sets into segments that are characteristic for particular modes. The algorithm finds the number of mode changes, detects their locations and infers the open probabilities of the modes. We apply our approach to data from the inositol-trisphosphate receptor (IP$_3$R). Based upon these results we propose that mode changes originate from alternative conformational states of the channel protein that determine a certain level of channel activity.

1. Introduction

Ion channels are proteins that regulate the flow of ions across the cell membrane by stochastic opening and

closing of a pore. When Neher and Sakmann [46] developed the patch-clamp technique it became possible to observe opening and closing of a single ion channel. In patch-clamp experiments, an electrode is moved close to of an ion channel so that electrical currents flowing through the channel can be measured. Because electrical currents indicate movement of charges through the channel pore, these data can be used for determining if ions flow through the channel—if a small (positive or negative) current is detected the channel is open whereas a zero current indicates that it is closed. Thus, neglecting fluctuations due to measurement noise, single ion channel data consist of a sequence of stochastic jumps between two or more currents (conductance levels) that correspond to the channel being open or closed.

Soon after single channel data became available, Colquhoun and Hawkes developed a mathematical framework for modelling stochastic time series of open and closed observations with aggregated continuous-time Markov model, see Colquhoun and Hawkes [10] for a very readable introduction. In the context of ion channel modelling, the time series of open and closed observations is represented by an aggregated Markov model which describes stochastic transitions between one or more open and closed that are connected to a directed graph. An aggregated Markov model not only provides a suitable statistical representation of ion channel kinetics but it also suggests a biophysical interpretation: opening and closing of the ion channel requires complex rearrangements of the three-dimensional structure of the channel protein known as conformational changes. Thus, it is tempting to speculate that transitions between states in the Markov model correspond to conformational changes of the channel protein. Moreover, the transition rates describing how fast transitions between adjacent states occur can be interpreted as the rates of chemical reactions that induce transitions between conformations of the channel protein associated with these states. Following this idea, modellers have attempted to represent the effects of all ligands, i.e. compounds that are known to interact with the channel, via corresponding state transitions. Because channels often have several different ligands that may each bind to the channel multiple times at different binding sites, this modelling approach has obvious practical limitations because it requires introducing a large number of open and closed states that are a priori indistinguishable by observing a time series of open and closed events. Nevertheless, if not applied dogmatically, the principle of relating the states of an aggregated Markov model to underlying structural changes at the level of the channel protein certainly has heuristic value and explains the popularity of these models in the context of ion channels.

There is a large body of literature dealing with the problem of inferring parameters of aggregated Markov models from given single channel data sets. In the early days of ion channel modelling, model fitting was based on a qualitative approach. Open and closed time distributions were calculated from a given Markov model [10] and fitted to empirical open and closed time histograms of the data. Because open and closed time distributions were parametrised by the rate constants of the Markov model, the model parameters could be determined by this fit. Horn and Lange [32] were the first to propose a quantitative approach to model fitting based on a likelihood function. But it took until the 1990s when sufficiently fast computers became available that these statistical methods were implemented for practical applications. First, approaches based on maximum likelihood estimation (MLE) were developed—the two most widely-used methods have been implemented in the software packages QuB [49, 50] and HJCFIT [11]. Rather than estimating the most likely set of rate constants, Markov chain Monte Carlo (MCMC) gives a more comprehensive view of uncertainty and correlations of model parameters by sampling from the posterior distribution. Ball et al. [2] developed the first MCMC algorithm for ion channel modelling, soon followed by Rosales [52], Rosales et al. [53] who inferred a discrete-time Markov model for the transitions between consecutive measurements. The method developed in Gin et al. [23], Siekmann et al. [59, 61] infers a continuous-time Markov model from a sequence of discrete measurements. Moreover, Hodgson [30], Hodgson and Green [31] applied reversible jump MCMC (RJMCMC) to the challenging task of model selection. See Calderhead et al. [5], Gin et al. [24] for recent reviews on modelling single-channel data with Markov models.

Aggregated Markov models provide good representations of ion channel kinetics at the fast timescale of consecutive channel openings and closings. However, there is increasing evidence that many ion channels primarily adjust their activity at a slower time scale, a phenomenon known as modal gating. In the broadest sense, modes are defined as different levels of activity between which the channel switches instantaneously. Thus, modes are at a slower timescale than individual openings and closings, apparently the notion was developed when it became clear that classes of bursts showed similar typical characteristics such as intraburst open probability and the average open time within a burst. In addition to different bursts we will also denote quiescent periods as a mode. Until today, neither burst nor modes have clear general definitions. Authors usually decide ad hoc which patterns observed in a data set are denoted bursts (for example, based upon a certain number of observed subsequent openings). Another possibility is to rely on a representation of the data set by a model and define bursts as sojourns in a subset of the model states [10].

One aim of the study presented here is to provide a statistical method that allows to identify instantaneous changes of open probability in single-channel data sets. By identifying the locations where the channel activity seems to switch to a different level of activity we take the most general point of view on modal gating—we divide data sets in segments that are characterised by significantly different open probabilities. This allows us to define mode changes in a relatively objective way—instead of requiring that observing a certain sequence of events constitutes a burst, we represent all relevant assumptions by specifying priors and likelihood of a Bayesian statistical model. Thus, for a given data set our method produces a segmentation where each segment is characterised by its open probability. The sequence of inferred open probabilities clearly shows if the channel indeed alternates between different levels of activity. If indeed clear levels of open probabilities can be identified it seems justified to say that the associated segments are representative for a particular mode. Therefore we define a mode as a recurring level of activity and we say that a data segment is representative for a mode if the average open probability within the segment is significantly different than the average open probability of adjacent segments. All quantities that are inferred by this method—the number of changepoints for a given data set, their locations, and the open probabilities within segments—are given as probability distributions. Thus, for each segment we know how uncertain the location of its boundaries are and we can therefore answer clearly in which mode the channel is at the resolution of individual data points.

Mode changes have been observed in many ion channels, the earliest example is perhaps from a classical study of the BK channel [39, 40], later continued by McManus and Magleby [41] and Rothberg et al. [55]. But modal gating was also found in other K^+ channels [7, 8, 9, 12, 16, 62, 67], Cl^- channels [4, 6], Na^+ channels [34], various Ca^{2+} channels [14, 15, 35, 38, 68], NMDA [47, 48], nicotinic receptors [1, 43, 45], and the RyR [19, 54, 69, 70]. In inositol-trisphosphate receptors (IP$_3$R), modes have been discovered only relatively recently: Ionescu et al. [36] found three levels of activity—high, intermediate and low—in a data set collected from type I IP$_3$R. Each mode is associated with a characteristic average open probability P_O which was found to be close to zero (low), approximately 30 % (intermediate) and approximately 70 % (high activity). This result is particularly interesting because the algorithm for segmenting a data set into modes presented by Ionescu et al. [36] (like the algorithm presented here) makes no explicit assumption on the average open probability within a mode. The fact that all three modes can be observed over a wide range of ligand concentration led to the hypothesis that the IP$_3$R is primarily regulated by modal gating: To adjust its behaviour, the IP$_3$R has to switch between three ligand-independent modes—regulation to an average activity level appropriate for a given ligand concentration is thus achieved by adjusting the time spent in each of the three modes.

A second goal of this study is to apply our method for analysis of modal gating to the IP$_3$R data set by Wagner and Yule [66]. We analyse data from type I and type II IP$_3$R at high inositol-trisphosphate (IP$_3$) and adenosine-trisphosphate (ATP) and several concentrations of

calcium which allows us to investigate the calcium dependency of modal gating. We apply a—to our knowledge—new statistical method for detecting mode changes in single-channel data sets. Previously used approaches are often based on calculating averages of statistical indicators of channel activity within a "window" of a certain number of data points. One problem with moving averages is that—depending on the window size—instantaneous jumps are transformed to gradual transitions so that changepoints cannot be localised very accurately. Also due to averaging we implicitly define the minimum distance between changepoints as the window size. Robustness of the results can be improved by varying the window size but it is not clear how to do this optimally. The algorithm by Ionescu et al. [36] localises changepoints at specific data points which is an improvement over methods based upon moving averages. Instead of estimating open probabilities in the neighbourhood of a data point, Ionescu et al. [36] distinguish activity levels based upon the length of bursts. The first step is a burst analysis [39]—short closings that are assumed too fast to arise due to ligand bindings are removed from the experimental trace. After burst analysis, the trace is assumed to consists of "bursts" and "burst-terminating gaps". Mode changes are determined in a second step by determining if burst length t_b or length of burst-terminating gaps t_g cross previously-defined thresholds T_b and T_g from above or below. This step assigns each mode change to a specific point in time so that a segmentation of the trace based upon different characteristic burst durations is obtained. In a third step, segments are classified by the length of bursts t_b and burst-terminating gaps t_g relative to the thresholds. Long bursts interspersed with short burst-terminating gaps ($t_b > T_g$, $t_g \leq T_g$) are regarded as characteristic for high channel activity whereas short bursts alternating with long burst-terminating gaps ($t_b \leq T_b$, $t_g > T_g$) suggest that the channel is in a mode of low activity. If bursts and burst-terminating gaps were both short ($t_b \leq T_b$, $t_g \leq T_g$), channel activity was considered intermediate. Segments where both thresholds were exceeded were only rarely observed—here, Ionescu et al. [36] assumed that the channel was undergoing a transition from the highly active mode to the inactive mode or vice versa. Following this procedure, Ionescu et al. [36] are indeed able to localise mode switching at a data point. However, the locations of changepoints are determined by a set of heuristic rules that have been carefully tested by Ionescu et al. [36] but ultimately it remains nevertheless unclear on which basis a changepoint is placed at a specific data point and what the uncertainty of this location is. Also, this method seems to assume implicitly three different modes of channel activity defined by the durations t_b and t_g relative to their thresholds T_b and T_g.

Changepoint problems, in particular for standard distributions such as binomial distributions have been studied statistically for a long time: The first references describing inference of a single change point seem to be Hinkley [28] and Hinkley and Hinkley [29]. A Bayesian approach for inferring a single changepoint as well as the parameters of binomially-distributed probabilities was published by Smith [63]. It is straight-forward to generalise these studies to an arbitrary but fixed number of changepoints. But because we have no a priori information on the number of changepoints in a trace it is additionally assumed that the exact number k of changepoints is unknown. In Sections 2 and 3 we develop a Bayesian framework for the inference of the number of changepoints k, a vector **j** of changepoint locations, and a vector **p** of open probabilities for the segments defined by **j**.

The main difficulty of this model is that (since the number of changepoints k is variable) the dimension of the probability space changes. An important tool for dealing with this problem is reversible jump Markov chain Monte Carlo (RJMCMC) developed by Green [26]. In this paper the author proposed a RJMCMC sampler for an unknown number of changepoints in a Poisson process. We adapt this method for the similar Bernoulli process; the moves of the MCMC sampler are described in Appendix A. An alternative approach to using MCMC for changepoint problems is direct sampling from the posterior distribution using the algorithm by Fearnhead [18]. Although it is, in principle, easier to implement this approach, we were unsuccessful in achieving sufficient efficiency for handling long single-channel data sets with usually more than a million of data points.

In Section 4 we apply the MCMC sampler to IP$_3$R data. Mostly, the observations made in previously published studies by Ionescu et al. [36] and Siekmann et al. [60] are confirmed. However, the more solid statistical basis of the method used here justifies a higher degree of confidence in the results—as previously mentioned, every quantity that is estimated is associated with a measure of its uncertainty because it is represented as a probability distribution.

In the discussion (Section 5) we give a general interpretation of the physiological role of modal gating. Although modal gating seems to be common in a wide range of ion channels, it is often difficult to find a physiological role for this wide-spread phenomenon. Therefore we suggest that modal gating may be caused by constraints that are imposed by the underlying molecular architecture of the channel protein. In this interpretation, each level of activity (mode) corresponds to a conformation of the channel which is associated with a certain level of activity. Ligand binding can only influence the relative frequency of the modes that the channel is found in rather than modulate the short-term kinetics of individual openings and closings, see Ionescu et al. [36]. Thus, mode switching is necessary so that the channel is able to exhibit intermediate levels of activity by switching between pre-defined ligand-independent kinetics determined by the modes. This conceptual model is consistent with what is known about modal gating in the IP$_3$R and a recent study of a bacterial potassium channel (KscA) that combines electrophysiology with mutation experiments and modelling gives additional support for this hypothesis.

2. Changepoint analysis of a Bernoulli process

We consider a sequence Y of N data points. It is assumed that channel currents at each data point have been classified as open or closed. For our data set from the inositol-trisphosphate receptor we classified currents below half of the average open current $\bar{I}_O$ as closed and currents above this threshold as open. We have found this approach for dealing with noise to be sufficient when we developed a Markov model for the same data set [60, 61]. In the application considered here, occasional misclassification of events should be even less important because the modes depend on the frequency of observed open and closed events rather than their exact sequence. Nevertheless, it would be possible to combine the method presented in the following with one of many available more sophisticated methods for idealising channel currents [3, 13, 20, 21, 33, 64, 65]. Thus—after appropriate treatment of noise in the channel currents—at each data point $y(n)$, for $n = 1, \ldots, N$ we observe binary events 0 or 1 or, in the case of an ion channel, open (O) or closed (C) events. We assume that at each position n an open event is observed with probability $p_O(n)$ and that $p_O(n)$ is independent of any observations made previously. We introduce the random variable $O(n)$ that gives the total number of open observations until index n in the trace Y.

Thus, if an ion channel opens with the same open probability p_0 for the whole sequence of data points Y, the probability of Y given the probability p_0 is

$$\mathbb{P}(Y|p_0) = p_0^{O(N)}(1 - p_0)^{N - O(N)} \tag{2.1}$$

Let us now assume that the open probability p_0 jumps to a different value p_1 at a changepoint j_1. Then the probability of the data Y is given by

$$\mathbb{P}(Y|p_0, p_1, j_1) = p_0^{s_0}(1 - p_0)^{u_0} p_1^{s_1}(1 - p_1)^{u_1}. \tag{2.2}$$

where $s_0 = O(j_1)$, $s_1 = O(N) - O(j_1)$ denote the number of open observations or "successes" observed and $u_0 = j_1 - O(j_1)$, $u_1 = N - j_1 - [O(N) - O(j_1)]$ stand for the number of closed observations or "failures" observed in the two segments (before and after the changepoint j_1) of the data.

For a number of k changepoints we generalise (2.2) to

$$\mathbb{P}(Y|\mathbf{p}, \mathbf{j}, J = k) = \prod_{i=0}^{k} p_i^{s_i}(1 - p_i)^{u_i}. \tag{2.3}$$

Here, $\mathbf{p}$ and $\mathbf{j}$ are the vectors of average open probabilities and changepoint positions and the condition $J = k$ means that the number of changepoints is assumed to be k. The numbers of successes s_i and failures u_i are calculated by

$$s_i = O(j_{i+1}) - O(j_i), \qquad (2.4)$$

$$u_i = j_{i+1} - j_i - [O(j_{i+1}) - O(j_i)], \qquad (2.5)$$

for $i = 1, \ldots, N$, and we define $j_0 = 0$ and $O(j_0) = 0$ as well as $j_{k+1} = N$.

Based upon the likelihood given in (2.3) our goal is to infer for a given data set Y the positions of change points $\mathbf{j}$ and the "success" probabilities $\mathbf{p}$. We further assume that the number of changepoints J is unknown a priori.

3. Bayesian inference of changepoints

Following a Bayesian statistics approach, these inference problems lead to studying the probability distribution $\mathbb{P}(\mathbf{p}, \mathbf{j}, J|Y)$ which can be rewritten according to Bayes' theorem

$$\mathbb{P}(\mathbf{p}, \mathbf{j}, J|Y) \propto \mathbb{P}(Y|\mathbf{p}, \mathbf{j}, J) \qquad (3.1)$$
$$\times \rho(J = k|\lambda)\pi_{J=k}(\mathbf{j} = (j_1, \ldots, j_k))\sigma_{J=k}(\mathbf{p} = (p_0, \ldots, p_k)|\alpha, \beta).$$

Here, '$\propto$' indicates that left and right hand side of equation (3.1) are equal up to a normalising constant. We also assume that given J, the vector of changepoints $\mathbf{j}$ and the vector of probabilities $\mathbf{p}$ are independent and moreover, that under the same condition the p_i are independent. The probability distributions ρ, $\pi_{J=k}$, and $\sigma_{J=k}$ are named priors and allow us to incorporate assumptions on the parameters J, $\mathbf{j}$ and $\mathbf{p}$. The subscripted $J = k$ for the prior $\pi_{J=k}$ indicates that this prior is conditional on the number J of changepoints, the prior parameters λ, α and β will be explained below.

Before we state the priors (that are chosen analogously to [18, 26]) we would like to mention that for given locations of changepoints $\mathbf{j}$ the probabilities $\mathbf{p}$ can be sampled directly if we choose a conjugate prior [51]. Choosing a beta prior $\sigma^i(p_i|\alpha_i, \beta_i) = B(\alpha_i, \beta_i)$ for each parameter $p_i \in (0, 1)$ appearing in the likelihood (2.3) ensures that the marginal posteriors for the p_i are also distributed according to a beta distribution:

$$\mathbb{P}(p_i|\mathbf{j}, J, Y) = B(s_i + \alpha_i, u_i + \beta_i). \qquad (3.2)$$

Thus, for given locations $\mathbf{j}$ the probabilities $\mathbf{p}$ can be sampled directly from (3.2) which facilitates the design of a Markov chain Monte Carlo (MCMC) sampler described in detail in Appendix A. Here we complete the description of our Bayesian statistics model by stating the priors. These priors are discussed in more detail in Section 5.1 of the Supplementary Information including possible alternative choices.

(a) Prior for the number J of changepoints

As Green [26] and Fearnhead [18] we assume that the number J of changepoints is distributed according to a Poisson distribution with mean λ.

$$\rho(J = k|\lambda) = e^{-\lambda}\frac{\lambda^k}{k!}. \qquad (3.3)$$

This prior penalises unrealistically high numbers J of changepoints that are much higher than λ while remaining flexible enough to accomodate larger numbers of changepoints. We chose $\lambda = 3$ used by Fearnhead [18], Green [25, 26] for a very similar application. As in these publication we condition on $k \leq k_{\max}$, we chose $k_{\max} = 1000$ (we obtained numbers of changepoints ranging from 20 to more than 600).

(b) Prior for the distribution of changepoints

Green [26] proposes an elegant prior that ensures that change points are not located too close to each other by assuming that the $\mathbf{j}$ are distributed according to an even-numbered uniform order statistics. Thus, we obtain

$$\pi_{J=k}(\mathbf{j} = (j_1, \ldots, j_k)) = \frac{1}{C_k} \prod_{i=0}^{k} (j_{i+1} - j_i - 1), \tag{3.4}$$

where

$$C_k = \binom{N-1}{2k+1}$$

is the number of combinations of picking $2k+1$ from $N-1$ numbers.

(c) Prior for open probabilities

As mentioned above we choose $\sigma_{J=k}(\mathbf{p}|\alpha, \beta)$ as a product of beta distributions that are conjugate to the Bernoulli factors appearing in (2.3):

$$\sigma_{J=k}(\mathbf{p}|\alpha, \beta) = \prod_{i=1}^{k} \sigma^i(p_i|\alpha_i, \beta_i) \tag{3.5}$$

where

$$\sigma^i(p_i|\alpha_i, \beta_i) = B(\alpha_i, \beta_i) = \frac{\Gamma(\alpha_i + \beta_i)}{\Gamma(\alpha_i)\Gamma(\beta_i)} p_i^{\alpha_i-1}(1-p_i)^{\beta_i-1}, \quad p_i \in (0,1). \tag{3.6}$$

and $\alpha = (\alpha_1, \ldots, \alpha_k)$, $\beta = (\beta_1, \ldots, \beta_k)$. All α_i, β_i must be positive. We chose $\alpha_i = \beta_i = 1$ for $i = 1, \ldots, k$ so that the marginal priors σ^i for each p_i reduce to the uniform distribution.

4. Results

(a) Changepoints in single-channel data from type I and type II IP$_3$R

The RJMCMC sampler described in Appendix A was run on data sets from IP$_3$R at high concentrations of IP$_3$ and ATP (10 μM IP$_3$, 5 mM ATP). These data are part of a comprehensive study of type I and type II IP$_3$R under various concentrations of IP$_3$, ATP and calcium, more details can be found in Wagner and Yule [66]. We ran the algorithm for many iterations ranging from 10^7 up to $5 \cdot 10^8$ iterations using the convergence plot for the number k of changepoints for convergence assessment. Because convergence diagnostics for RJMCMC samplers is not a simple task we were conservative and for many data sets running the sampler for much less iterations would probably have been sufficient. Another advantage of running many iterations is that a good idea of alternative segmentations for different numbers of changepoints can be obtained instead of only attempting to resolve the "most likely" number of changepoints by sufficiently many samples.

The probability distribution $\mathbb{P}(\mathbf{p}, \mathbf{j}, J|Y)$ approximated by the RJMCMC sampler answers several questions at once.

  (i) The marginal distribution $\mathbb{P}(J = k|Y)$ shows how many changepoints are found in the data Y.

 (ii) The marginal distribution $\mathbb{P}(\mathbf{j}|J = k, Y)$ gives the locations of the changepoints under the condition that there are k changepoints.

(iii) From the marginal distribution $\mathbb{P}(\mathbf{p}|J = k, Y)$ we obtain the open probabilities within each of the $k+1$ segments.

In the following we will use these probability distributions for answering the following questions:

(i) Can we confidently claim that the IPR exhibits mode changes? This question will be answered by examining subsequent components p_i and p_{i+1} in the vector $\mathbf{p}$ for a given number of changepoints k. If p_i and p_{i+1} alternate between clearly different levels, for example, if p_i is "low" then p_{i+1} is "high", this is taken as evidence for mode switching.

(ii) How many distinct modes can be observed? Does the channel simply switch between "high" and "low" activity (which are both associated with similar open probabilities)? Or can one or more levels of intermediate activity be found?

(iii) For a certain number of changepoints k, how sure can we be about their locations? This question can be answered by the marginal distribution of $\mathbf{j}$.

(iv) Using the distribution of differences between subsequent changepoints $\Delta_i = j_{i+1} - j_i$ we can determine how much time τ_i the channel spends in each of the modes found previously.

(v) The distribution of the sojourn times τ_i indicates how variable sojourns in each of the modes are.

(vi) Finally, the distribution of the number of changepoints J together with the previous distributions, clearly indicates how much can be inferred about the changepoints for a given data set. If the number of changepoints J is spread over a considerable range, and if the locations $\mathbf{j}$ are characterised by large standard deviations and/or multi-modality, this suggests that for these data, changepoints cannot be analysed very well.

Most of these questions cannot be answered confidently or cannot be answered at all by the heuristic algorithm described by Ionescu et al. [36] or approaches based upon moving averages like in Siekmann et al. [60].

(b) Does the IPR exhibit mode changes?

For all calcium concentrations, the open probabilities of subsequent segments alternate between low and high values. Histograms of the open probabilities show that the channel switches between one inactive mode characterised by an open probability close to zero and an active mode with an open probability of approximately 70% (Figure 1).

Interestingly, for $1000\,\text{nM}$ Ca^{2+}, type I IP$_3$R shows some evidence for a third mode at probabilities between 20-30% which has also been observed by Ionescu et al. [36] who reported a mode of intermediate activity for their type I IP$_3$R data set (Figure 1a). No intermediate activity is found for type II IP$_3$R data although in general results for both receptor types are very similar.

(c) How frequently does mode switching occur?

A first result that can be gained at the global level is a relationship of average channel activity and frequency of mode switching. We choose the average open probability p_O as a measure of channel activity and plot it against the number of mode changes per second (Figure 2). For more detail on the absolute number of mode changes that were inferred for data sets of different lengths, see Section 6 in the Supplementary Information.

The number of mode changes were calculated by dividing the total number of changepoints that were inferred for a data set by the number of data points—this yields the number of changepoints per data point. The number of changepoints per second was then calculated by dividing by the sampling interval $\tau = 0.05\,\text{ms}$. The plot shows that at a high level of activity there are relatively few mode changes—the channel spends most of the time in the highly active mode whereas the inactive mode is essentially suppressed. In contrast, for lower open probabilities p_O the number of mode changes per second increases up to a factor of four. This shows that even at low open probabilities the highly active mode is visited for very short intervals which indicates
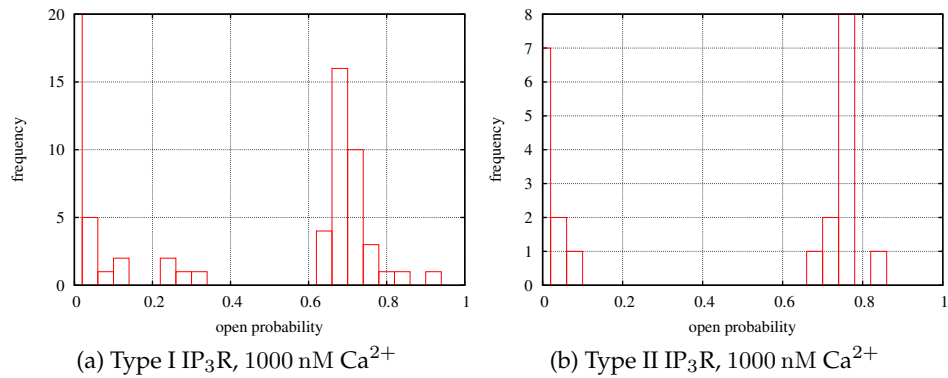
(a) Type I IP$_3$R, 1000 nM Ca^{2+} (b) Type II IP$_3$R, 1000 nM Ca^{2+}

Figure 1: Histogram of the mean values of the probabilities **p** at 1000 nM Ca^{2+} for type I IP$_3$R and type II IP$_3$R (10 μM IP$_3$, 5 mM ATP). The distributions are clearly bi-modal with peaks at open probabilities of about zero and 70%. Also for other concentrations the distribution is clearly bi-modal. This indicates that the IP$_3$R switches between two modes characterised by low open probability of nearly 0% and high open probability of 70%. Only for type I IP$_3$R and only at the calcium concentration shown here, there is some evidence for an intermediate level of activity of 20-30%.
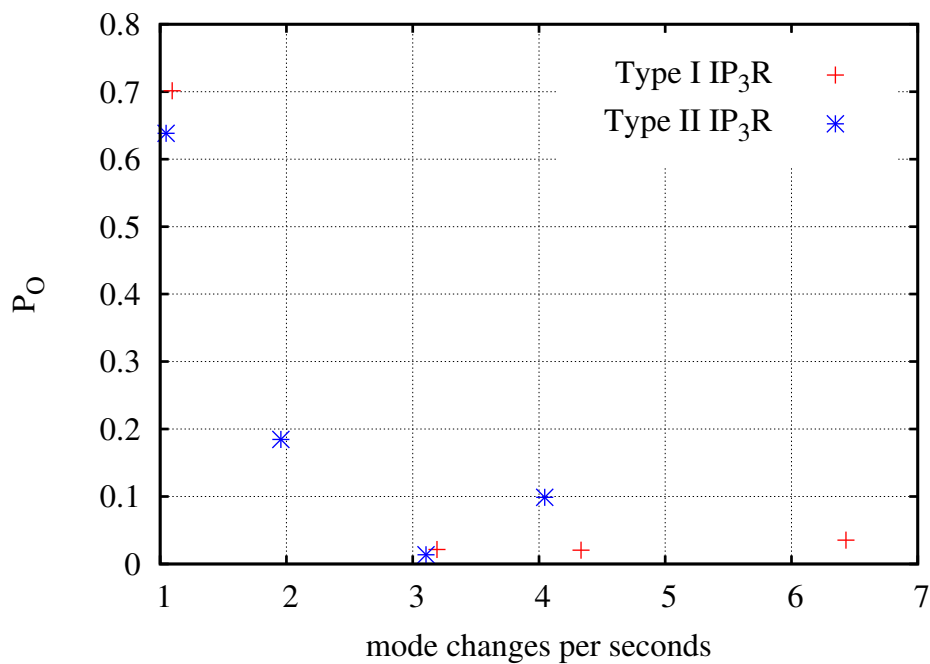

Figure 2: Average open probabilities p_O for observed numbers of mode changes per second.

that it is harder to switch off the active mode than the inactive mode. The relationship between mode changes per second and level of activity is very similar for type I and type II IP$_3$R.

(d) How uncertain are the locations of changepoints?

For a number k of changepoints the probability distribution $\mathbb{P}(\mathbf{j}|J=k,Y)$ allows us to explore where these changepoints are located. If the number of changepoints per second is low, the positions of the changepoints are usually well-fixed (Figure 3).
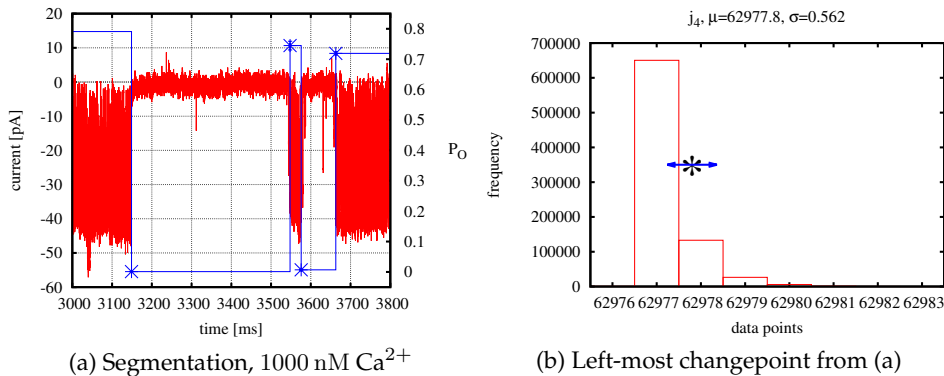

Figure 3: (a) Part of a segmentation of a single-channel data set. Channel currents are plotted in red. The changepoint locations are indicated by blue asterisks '*', their level corresponds to the open probability in the segment following the changepoint. Bars indicating standard deviations of the inferred changepoint locations (horizontal direction) and for the open probabilities (vertical direction) are provided but they are too small to be seen. (b) Probability distribution of the first changepoint j_4 of the segmentation shown in (a). The changepoint approximately lies at data point 62,978. For a sampling interval $\tau = 0.05\,\mathrm{ms}$ this is consistent with a time point of roughly $3,150\,\mathrm{ms}$, cf. (a). (For reference to colour, refer to the online version of this article).

As the density of changepoints increases, the distribution of changepoint locations becomes multi-modal. This indicates that two or more alternative configurations of changepoints are consistent with the observed data, or, in other words that for a given number of changepoints, different segmentations of the trace in active and inactive segments are possible.

An example is shown in Figure 4. The changepoint j_{21} either marks the end of a short segment of only 60 data points (Figure 4b) or is located at the end of a long segment of about 8,700 data points. Depending on the two alternative locations, the open probability within the segment between j_{20} and j_{21} is either approximately 20% or only 0.2%. There is overwhelming support for the second location of j_{21}—only in 300 samples, the short segment with $p_{20} \approx 20\%$ is obtained whereas in more than 2 millions of the samples the long segment with $p_{20} \approx 0.2\%$ appeared.

Although there is little support for inserting a short segment of intermediate open probability, the bimodal distribution of a changepoint introduces bimodality also in the distributions of subsequent changepoint locations and open probabilities. In the example shown in Figure 4, placing changepoint j_{21} close to j_{20} (Figure 4b) inserts a segment with an open probability of $p_{20} \approx 20\%$ followed by a segment with a low open probability p_{21} close to zero. In contrast, if j_{21} is located further apart (Figure 4d), the subsequent segment has a high open probability p_{21} which means that the distribution $\mathbb{P}(p_{21}|J=k,Y)$ is bimodal. Fortunately, it is easy to separate the two modes of $\mathbb{P}(p_{21}|J=k,Y)$ because the open probabilities are concentrated at values close to zero or close to 70%. This allows us to select the samples that are representative for a long segment between j_{20} and j_{21} by thresholding. Selecting a specific configuration of changepoints enables us to study sojourn times in the inactive and the active mode.
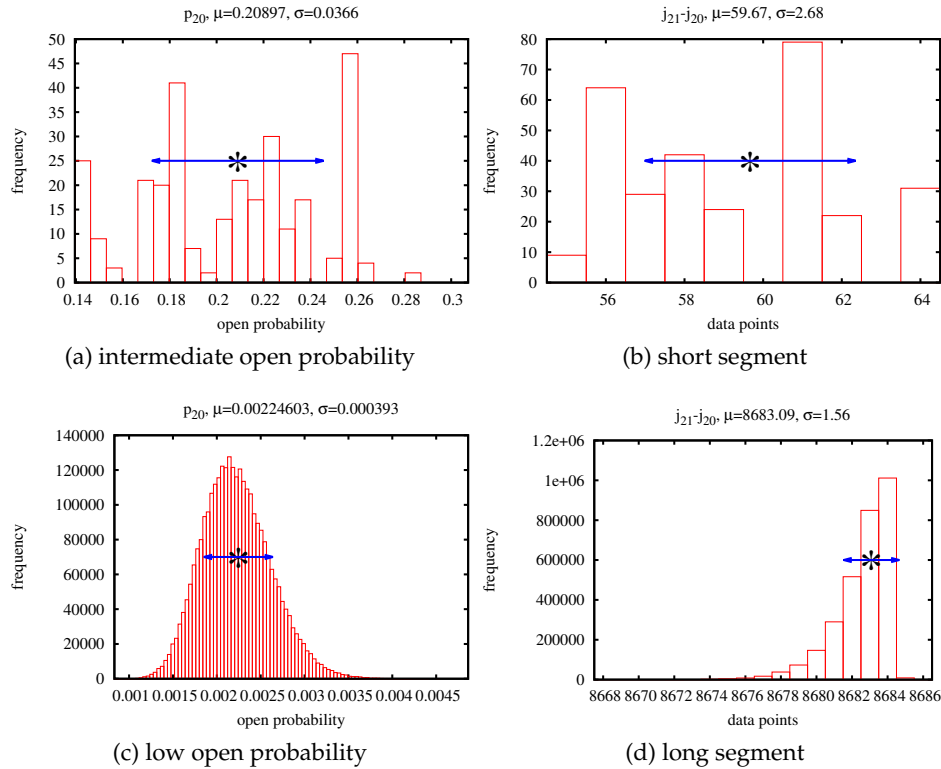
Figure 4: Alternative configurations of changepoints are caused by short visit to an intermediate level of activity. (a) Histogram for the open probability inferred for a short segment between j_{20} and j_{21}. (b) Histogram of the segment length for the segment between j_{20} and j_{21}. Both histograms are supported only by a small number of samples. (c) and (d) show open probability and segment length for the alternative position j_{21} which results in a long segment with low open probability. This configuration has overwhelming support over the alternative shown in (a), (b).

(e) What is the distribution of sojourn times in modes?

In the preceding sections we have presented evidence that the IP$_3$R switches between two modes which we have previously named [60], in analogy to gears of the automatic transmission of cars the inactive "park" mode and the highly active "drive" mode. We now investigate the distribution of sojourn times in these two modes. For this purpose we calculate the distributions of differences of subsequent changepoints $\Delta_i = j_{i+1} - j_i$ (see Figures 4b, 4d for examples). If p_i is close to zero, Δ_i is considered as the sojourn within the inactive mode and denoted Δ_i^{park}, whereas, if p_i is high. i.e. approximately 70%, Δ_i is the sojourn in the highly active mode and denoted $\Delta_i^{\mathrm{drive}}$. Because data points are separated by the sampling interval $\tau = 0.05\,\mathrm{ms}$, the sojourn times can simply be calculated by $\tau_i^{\mathrm{park}} = \Delta_i^{\mathrm{park}}\tau$ and $\tau_i^{\mathrm{drive}} = \Delta_i^{\mathrm{drive}}\tau$. Sojourn time histograms are constructed from the mean values $\bar{\tau}_i^{\mathrm{park}}$ and $\bar{\tau}_i^{\mathrm{drive}}$.

The results are shown in Figures 5 and 6. Sojourn times in both modes varied over a wide range so that a logarithmically-spaced histogram was used. Moreover, histograms over a logarithmic time scale give a representation that is especially suitable if sojourn time distributions are mixtures of exponential distributions. Logarithmically-spaced histograms of mixtures of exponential distributions have local maxima at the time constants of the exponentials, see Keener and Sneyd [37] for an illustrative explanation. It is usually assumed that open and closed time distributions of ion channels are distributed according to a mixture of exponentials.

For the results presented here it is unclear if also the distribution of sojourn times in active and inactive mode are consistent with a mixture of exponentials. Although on visual inspection it seems that the histograms could arise from one or a mix of a few exponential components, actual fits to mixtures of exponentials are unsatisfactory (results not shown). However, even data sets with many mode changes only provide us with at most a few hundred sojourn times in each mode so that it seems unjustified to dismiss an exponential mixture distribution on this basis.

It is important to note here that, to the best of our knowledge, none of the existing approaches for the analysis of modal gating is capable of reliably calculating sojourn distributions in different modes. Estimating the positions of mode changes by moving average is inevitably imprecise because instantaneous jumps from one level activity to another are transformed to gradual transitions. In contrast, the algorithm by Ionescu et al. [36] gives changepoint locations at the resolution of single data points. But due to the heuristic nature of this method it is impossible to assess the uncertainty of the inferred changepoint locations.

5. Discussion

The statistical analysis of modal gating presented here, shows that the IP_3R switches between two levels of activity that preserve similar characteristics across a wide range of ligand concentrations. The results indicate that the IP_3R is limited to two extreme types of kinetics, thus, in analogy with the automatic transmission in a car we refer to the switching between these different levels of activity as "park-drive gating"—the inactive mode is characterised by a low average open probability $p_O^{\text{park}} \approx 0\%$ whereas the average probability of the active mode is $p_O^{\text{drive}} \approx 70\%$. Intermediate levels of activity can only be produced by "mixing" park and drive mode in a suitable way. This idea was introduced by Ionescu et al. [36] who proposed modal gating as the principal regulatory mechanism of the IP_3R. If this is indeed the case more generally—and as mentioned previously, many ion channels seem to exhibit modal gating—this strongly suggests that modelling of single-channel data which is currently mainly based on Markov models of the fast time scale of individual openings and closings should be complemented by a thorough analysis of modal gating as proposed in this paper.

It is tempting to interpret the fact that the IP_3R exhibits the same two modes for a wide range of experimental conditions as the effect of biophysical constraints. These constraints could arise at the structural level of the channel protein by two different conformations that exhibit the inactive or the active gating kinetics observed in the data. This idea was raised, for example, by Naranjo and Brehm [45] in a study of modal gating in the acethylcholine receptor. Such an interpretation would have important implications for the understanding of the regulation of ion channels. If modal gating is caused by switching between different conformations this implies that different ligand concentrations primarily influence how long the channel stays in each of the available conformations rather than modulate the short-term channel kinetics. Instead the short-term kinetics is completely determined by the conformation that the channel is in.

Further support for this hypothesis comes from a recent study of a bacterial potassium channel (KscA). Starting from an extensive electrophysiological study of KscA [8, 9] which exhibits four different modes (three different types of bursts and very long quiescent periods), Chakrapani et al. [7] then combined mutation studies, comparison of crystal structures of these mutants and molecular dynamics simulation for investigating the molecular basis of the different burst modes. Similar to the studies of IP_3R, the authors found that ligand binding (protons in the case of KscA) modulated the duration and frequency rather than changing the characteristics of the modes themselves.

Interestingly, substituting one particular site of the wild-type KscA channel protein in most cases abolishes the long quiescent periods and (depending on the substitution) stabilises one of the burst modes observed in the wild-type. Crystallographic studies and molecular dynamics modelling reveal that ion profile and water occupancy around the selectivity filter of the channel are changed and simulations indicate that mutations lead to stabilisation of one of a few
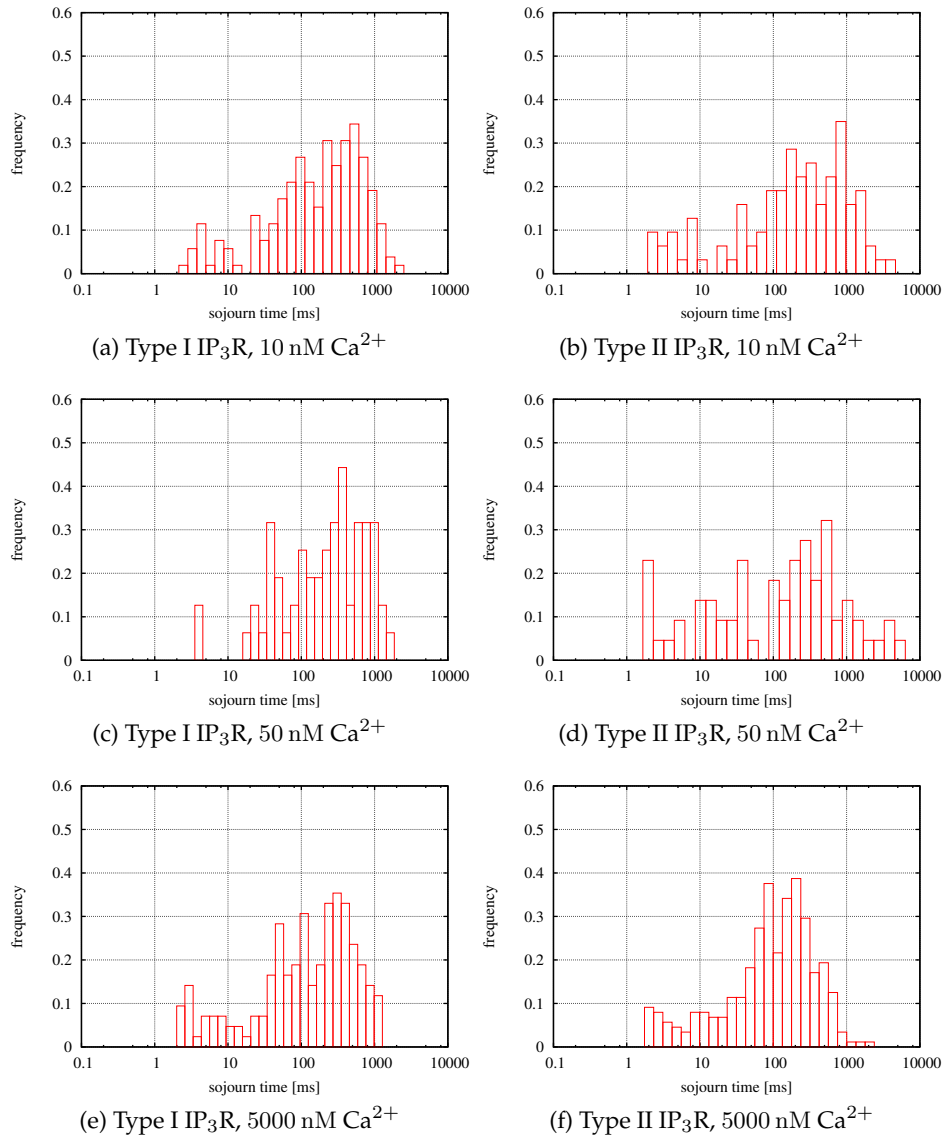
(a) Type I IP$_3$R, 10 nM Ca^{2+}

(b) Type II IP$_3$R, 10 nM Ca^{2+}

(c) Type I IP$_3$R, 50 nM Ca^{2+}

(d) Type II IP$_3$R, 50 nM Ca^{2+}

(e) Type I IP$_3$R, 5000 nM Ca^{2+}

(f) Type II IP$_3$R, 5000 nM Ca^{2+}

Figure 5: Sojourn time in park mode for type I and Type II IP$_3$R for various calcium concentrations.

alternative conformational states found in the wild-type. The authors conclude that each of the alternative conformational states is associated with the particular gating behaviour that is characteristic for the three types of bursts. In the wild-type, the channel switches between these conformations and shows three types of bursting behaviour as well as long quiescent periods.

Thus (under the assumption that also in the IP$_3$R conformational changes are exhibited at the kinetic level by modal gating) we come to the conclusion that the IP$_3$R responds to changes in ligand concentrations by adjusting the time the channel spends in the conformation associated with the park mode relative to the drive mode. In contrast, changes of ligand concentrations have little influence on the modulation of the short-term kinetics of openings and closings. This idea has been realised in a model by Siekmann et al. [60] that represented modal gating of the IP$_3$R by two ligand-independent models that were connected by ligand-dependent transition rates.
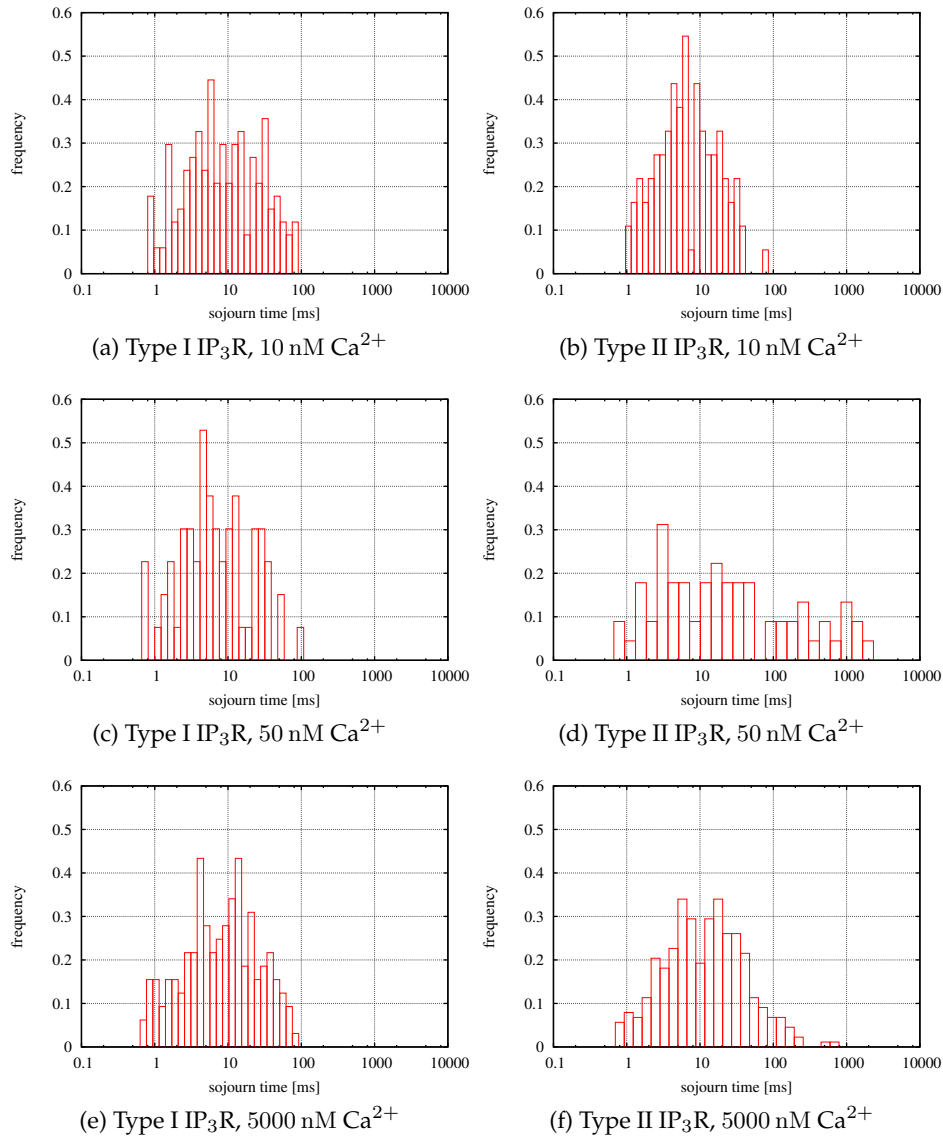
Figure 6: Sojourn time in drive mode for type I and type II IP$_3$R for various calcium concentrations.

The underlying construction principle of the conceptual model described here is opposite to the classical Monod-Wyman-Changeux (MWC) model [44]. Monod et al. [44] proposed a model structure where two alternative conformational states of an enzyme are modulated by ligand binding. Different affinities of the two conformations for a substrate increases the rate of binding for higher substrate concentration—an effect that is known as positive cooperativity. In this way the MWC model provides an explanation of positive cooperativity due to the asymmetric behaviour of two alternative conformations of a protein. It is important to note that transitions between the two alternative conformational states are independent of substrate concentrations. The MWC model is a popular structure for ion channel models, for example, an increasingly detailed model of the BK channel developed by Rothberg and Magleby [56, 57, 58].

The differences between our proposed model for modal gating in ion channels (ligand-independent modes whose transitions are regulated by ligand binding) and the classical MWC model for allosteric kinetics of enzymes (ligand-independent conformational changes whose behaviour is modulated by ligand binding) arise because of their different scopes. While the MWC model aims to explain how the rate of binding substrate is increased after binding the first substrate molecule, our model demonstrates how mode switching could originate from conformational changes. We make no assumption about the chemical details of ligand binding that may shape the ligand-dependency of mode switching. Indeed, we believe that this is a challenging question for future work which possibly may not be answered from single-channel data alone. Because mode changes are by definition observed on a slow time scale, even in data recorded over a long time only relatively few events are observed. This makes it hard to describe modal sojourn time distributions that span several orders of magnitude by a state-based model which describes ligand binding by mass action kinetics.

A. Reversible jump MCMC (RJMCMC) sampling of changepoints

In the following we will describe the moves of a Metropolis-Hastings sampler [27, 42] for sampling from the posterior distribution given $\mathbb{P}(\mathbf{p}, \mathbf{j}, J)$ in (3.1). Which move is chosen is determined by a mixing distribution. In a first step, it was decided with a probability $p_{\mathrm{change}J} = 0.5$ if the proposal shall alter the number of changepoints, i.e. if the birth or the death move is chosen. Similarly, provided that an alteration of the number of changepoints J is proposed, the birth move is carried out with a probability of $p_{\mathrm{birth}} = 0.5$ unless death is not possible ($J = 0$) or $J = k_{\max}$ so that the birth move would increase the number of changepoints above $k_{\max}$. Between shift and step move the smaller step move was chosen with $p_{\mathrm{step}} = 0.9$ because it was found that the sampler usually converged quickly towards a certain configuration of changepoints for which shift moves usually were not accepted because they propose too large steps.

(a) Shift move

For a given number $J = k$ of changepoints we simply need to propose $\mathbf{j}'$ from the current locations of changepoints $\mathbf{j}$. As mentioned above the proposal $\mathbf{p}'$ can be (according to (3.2)) generated by direct sampling. By doing a *shift* move we simply choose one of the changepoints j_i, $i = 1, \ldots, k$, and place it at a different location j_i' somewhere in $\{j_{i-1} + 1, \ldots, j_{i+1} - 1\}$. Thus, a proposal is generated in the following steps:

(i) Decide which j_i will be shifted by drawing i from the uniform distribution $U(1, k)$.
(ii) Draw a new position j_i' from $U(j_{i-1} + 1, \ldots, j_{i+1} - 1)$.
(iii) Proposals p_{i-1}', p_i' are generated by sampling from beta distributions:

$$p_m' \sim B(s_m' + \alpha_m, u_m' + \beta_m), \ m = i - 1, i,$$

where s_m' and u_m' are the successes and failures calculated for the proposed changepoint position j_i' and $\alpha_m = \beta_m = 1$ as stated in Section 3(c).

After a proposal (j_i', p_{i-1}', p_i') has been generated we have to decide if it is accepted as a sample from the posterior. For this purpose the acceptance ratio $r\{(\mathbf{j}', \mathbf{p}'), (\mathbf{j}, \mathbf{p})\}$ has to be calculated. Because the number of changepoints remains the same the priors for the number of changepoints ρ cancel out. The prior ratio for the location of changepoints is greatly simplified because only one location j_i is moved:

$$r_{\mathrm{shift}}^{\mathrm{prior}} = \frac{j_i' - j_{i-1} - 1}{j_i - j_{i-1} - 1} \times \frac{j_{i+1} - j_i' - 1}{j_{i+1} - j_i - 1}. \tag{A 1}$$

Analogously, also in the likelihood ratio many terms cancel out:

$$r_{\text{shift}}^{\text{L}} = \frac{(p'_{i-1})^{s'_{i-1}}[1-p'_{i-1}]^{u'_{i-1}}}{p_{i-1}^{s_{i-1}}[1-p_{i-1}]^{u_{i-1}}} \times \frac{(p'_i)^{s'_i}[1-p'_i]^{u'_i}}{p_i^{s_i}[1-p_i]^{u_i}} \tag{A 2}$$

As usual for Metropolis-Hastings algorithms, the proposal is accepted with probability

$$\alpha = \min\{1, r\}$$

where $r_{\text{shift}} = r_{\text{shift}}^{\text{prior}} \cdot r_{\text{shift}}^{\text{L}}$ is calculated from (A 1) and (A 2).

(b) Step move

The shift move may sometimes propose too large changes of a changepoint j_i that are unlikely to be accepted. Therefore, we add the step move, a symmetric uniform random walk with a step size d of a few data points (we usually used 5 data points in each direction), i.e. we draw a new position j'_i from $U(j_i - d, j_i + d)$. Otherwise we proceed as in (a), i.e. we sample new probabilities p'_m as described above and accept the proposal according to (A 1) and (A 2).

(c) Birth move

The birth move adds one changepoint, so in the proposal the number J' of changepoints is increased from k to $k+1$. Cases where the dimensionality of the parameter sets changes must be treated with caution—this is the reason why reversible jump MCMC was originally developed. In particular, the acceptance ratio for a birth move depends on a corresponding death move. Therefore, derivation of the acceptance ratio for birth and death move is postponed until Section (e).

The birth move consists of two steps, first we randomly choose an existing changepoint j_i before which the new changepoint j'_i is inserted. Then we sample a position j'_i within $\{j_{i-1}, \ldots, j_i\}$ analogously to the shift move described previously.

   (i) Draw i from the uniform distribution $U(1, k+1)$.
   (ii) Sample j'_i as in the shift move (if $i = k+1$, sample j'_{k+1} between j_k and $j_{k+1} = N$).
   (iii) Sample proposals p'_{i-1}, p'_i as in the shift move.

(d) Death move

The death move removes a randomly chosen changepoint.

   (i) Sample i from the uniform distribution $U(1, k)$.
   (ii) In $\mathbf{j}'$, remove j_i.
   (iii) In $\mathbf{p}'$, replace probabilities p_{i-1} and p_i by p'_i which is sampled from $B(s_{i-1} + s_{i+1} + \alpha_{i-1}, u_{i-1} + u_i + \beta_{i-1})$.

(e) Acceptance ratio for birth & and death move

We derive r_{birth} as first explained in Green [26] by considering a birth move and the corresponding death move that reverses adding the point j'_i. For a readable introduction to reversible jump MCMCM (RJMCMC), see Geyer [22] and Fan and Sisson [17].

First we consider the prior ratio

$$r_{\text{birth}}^{\text{prior}} = \frac{\rho(k+1)}{\rho(k)} \times \frac{\pi_{J=k+1}(\mathbf{j}')}{\pi_{J=k}(\mathbf{j})}. \tag{A 3}$$

Similarly to the shift move many terms cancel out. We only need to consider the ratio

$$r_{\text{birth}}^{\text{L}} = \frac{(p'_{i-1})^{s'_{i-1}}[1 - p'_{i-1}]^{u'_{i-1}}(p'_i)^{s'_i}[1 - p'_i]^{u'_i}}{p_{i-1}^{s_i}[1 - p_i]^{u_i}}. \tag{A 4}$$

The last component that we need to consider is the proposal ratio between birth and death move. This accounts for the fact that when adding a new changepoint, its position j'_i is sampled from a uniform distribution $U(j_{i-1} + 1, j_i - 1)$ (thus j'_i is sampled with probability $1/(j_i - j_{i-1} - 2)$) whereas we obviously have no choice of the position if we decide to remove j'_i again (i.e. here the position is j'_i with probability 1). This is accounted for by the proposal ratio

$$r_{\text{birth}}^{\text{proposal}} = \frac{1/(j_i - j_{i-1} - 2)}{1} = \frac{1}{(j_i - j_{i-1} - 2)}. \tag{A 5}$$

The acceptance ratio for the birth move is calculated by $r_{\text{birth}} = r_{\text{birth}}^{\text{prior}} \cdot r_{\text{birth}}^{\text{L}} \cdot r_{\text{birth}}^{\text{proposal}}$. The ratio r_{death} is found by considering a death move which is "balanced" by the corresponding birth move.

Acknowledgment

Data accessibility

The `C` code implementing the algorithm for mode change analysis described in this article has been released under the GNU General Public License, version 2 (GPLv2), and is available via `github`. The most current version can be obtained from https://github.com/merlinthemagician/icmcstat.git.

References

1 Auerbach, A. and Lingle, C. J. (1986). Heterogeneous kinetic properties of acetylcholine receptor channels in *xenopus* myocytes. *Journal of Physiology*, 378: 119–140.

2 Ball, F. G., Cai, Y., Kadane, J. B., and O'Hagan, A. (1999). Bayesian inference for ion-channel gating mechanisms directly from single-channel recordings, using Markov chain Monte Carlo. *Proceedings of the Royal Society of London A*, 455: 2879–2932.

3 Ball, F. G. and Sansom, M. S. P. (1989). Ion-channel gating mechanisms: Model identification and parameter estimation from single channel recordings. *Proceedings of the Royal Society of London B*, 236(1285): 385–416.

4 Blatz, A. L. and Magleby, K. L. (1986). Quantitative description of 3 modes of activity of fast chloride channels from rat skeletal-muscle. *Journal of Physiology-London*, 378: 141–174.

5 Calderhead, B., Epstein, M., Sivilotti, L., and Girolami, M. (2013). Bayesian approaches for mechanistic ion channel modeling. In M. V. Schneider (Ed.), *In Silico Systems Biology*, volume 1021 of *Methods in Molecular Biology* (pp. 247–272). Humana Press.

6 Catacuzzeno, L., Trequattrini, C., Petris, A., and Franciolini, F. (1999). Bimodal kinetics of a chloride channel from human fibroblasts. *Journal of Membrane Biology*, 170(2): 165–172.

7 Chakrapani, S., Cordero-Morales, J. F., Jogini, V., Pan, A. C., Cortes, D. M., Roux, B., and Perozo, E. (2011). On the structural basis of modal gating behaviour in K^+ channels. *Nature Structural and Molecular Biology*, 18(1): 67–75.

8 Chakrapani, S., Cordero-Morales, J. F., and Peroso, E. (2007a). A quantitative description of KscA gating II: Single-channel currents. *Journal of General Physiology*, 130(5): 479–496.

9 Chakrapani, S., Cordero-Morales, J. F., and Perozo, E. (2007b). A quantitative description of KscA gating I: Macroscopic currents. *Journal of General Physiology*, 130(5): 465–478.

10 Colquhoun, D. and Hawkes, A. G. (1981). On the stochastic properties of single ion channels. *Proceedings of the Royal Society of London B*, 211: 205–235.

11 Colquhoun, D., Hawkes, A. G., and Srodzinski, K. (1996). Joint distributions of apparent open and shut times of single-ion channels and maximum likelihood fitting of mechanisms. *Philosophical Transactions of the Royal Society of London A*, 354: 2555–2590.

12 Cooper, E. and Shrier, A. (1989). Inactivation of A currents and A channels on rat nodose neurons in culture. *The Journal of General Physiology*, 94: 881–910.

13 de Gunst, M. C. M., Künsch, H. R., and Schouten, J. G. (2001). Statistical analysis of ion channel data using hidden markov models with correlated state-dependent noise and filtering. *Journal of the American Statistical Association*, 96(455): 794–804.

14 Delcour, A. H., Lipscombe, D., and Tsien, R. W. (1993). Multiple-Modes of N-type calcium-channel activity distinguished by differences in gating kinetics. *Journal of Neuroscience*, 13(1): 181–194.

15 Delcour, A. H. and Tsien, R. W. (1993). Altered prevalence of gating modes in neurotransmitter inhibition of N-type calcium channels. *Science*, 259: 980–984.

16 Dreyer, I., Michard, E., Lacombe, B., and Thibaud, J. B. (2001). A plant shaker-like K^+ channel switches between two distinct gating modes resulting in either inward-rectifying or 'leak' current. *FEBS Letters*, 505: 233–239.

17 Fan, Y. and Sisson, S. A. (2011). Reversible jump MCMC. In S. Brooks, A. Gelman, G. L. Jones, and X.-L. Meng (Eds.), *Handbook of Markov Chain Monte Carlo*, Handbooks of Modern Statistical Methods chapter 3, (pp. 67–92). Boca Raton: Chapman & Hall/CRC, Taylor & Francis, 1st edition.

18 Fearnhead, P. (2006). Exact and efficient Bayesian inference for multiple changepoint problems. *Statistics and Computing*, 16: 203–213.

19 Fill, M., Zahradníková, A., Villalba-Galea, C. A., Zahradník, I., Escobar, A. L., and Györke, S. (2000). Ryanodine receptor adaptation. *The Journal of General Physiology*, 116: 873–882.

20 Fredkin, D. R. and Rice, J. A. (1992a). Bayesian restoration of single-channel patch clamp recordings. *Biometrics*, 48(2): 427–448.

21 Fredkin, D. R. and Rice, J. A. (1992b). Maximum likelihood estimation and identification directly from single-channel recordings. *Proceedings of the Royal Society B*, 249(1325): 125–132.

22 Geyer, C. J. (2011). Introduction to Markov Chain Monte Carlo. In S. Brooks, A. Gelman, G. L. Jones, and X.-L. Meng (Eds.), *Handbook of Markov Chain Monte Carlo*, Handbooks of Modern Statistical Methods chapter 1, (pp. 3–48). Boca Raton: Chapman & Hall/CRC, Taylor & Francis, 1st edition.

23 Gin, E., Falcke, M., Wagner, L. E., Yule, D. I., and Sneyd, J. (2009a). Markov chain Monte Carlo fitting of single-channel data from inositol trisphosphate receptors. *Journal of Theoretical Biology*, 257: 460–474.

24 Gin, E., Wagner II, L. E., Yule, D. I., and Sneyd, J. (2009b). Inositol trisphosphate receptor and ion channel models based on single-channel data. *Chaos: An Interdisciplinary Journal of Nonlinear Science*, 19(3): 037104.

25 Green, P. (2003). Transdimensional Markov Chain Monte Carlo. In P. Green, N. L. Hjort, and S. Richardson (Eds.), *Highly Structured Stochastic Systems*, volume 27 of *Oxford Statistical Science Series* (pp. 179–198). Oxford, New York: Oxford University Press.

26 Green, P. J. (1995). Reversible jump Markov chain Monte Carlo computation and Bayesian model determination. *Biometrika*, 82(4): 711–732.

27 Hastings, W. K. (1970). Monte-Carlo sampling methods using Markov chains and their applications. *Biometrika*, 57(1): 97–109.

28 Hinkley, D. V. (1970). Inference about the change-point in a sequence of random variables. *Biometrika*, 57(1): 1–17.

29 Hinkley, D. V. and Hinkley, E. A. (1970). Inference about the change-point in a sequence of binomial variables. *Biometrika*, 57(3): 477–488.

30 Hodgson, M. E. A. (1999). A Bayesian restoration of an ion channel signal. *Journal of the Royal Statistical Society: Series B (Statistical Methodology)*, 61(1): 95–114.

31 Hodgson, M. E. A. and Green, P. J. (1999). Bayesian choice among Markov models of ion channels using Markov chain Monte Carlo. *Proceedings of the Royal Society of London Series A-Mathematical Physical and Engineering Sciences*, 455(1989): 3425–3448.

32 Horn, R. and Lange, D. (1983). Estimating kinetic rate constants from single channel data. *Biophysical Journal*, 43: 383–404.

33 Hotz, T., Schütte, O. M., Sieling, H., Polupanow, T., Diederichsen, U., Steinem, C., and Munk, A. (2013). Idealizing ion channel recordings by a jump segmentation multiresolution filter. in press.

34 Howe, J. R. and Ritchie, J. M. (1992). Multiple kinetic components of sodium channel inactivation in rabbit Schwann cells. *Journal of Physiology*, 455: 529–566.

35 Imredy, J. P. and Yue, D. T. (1994). Mechanism of Ca^{2+}-sensitive inactivation of L-type Ca^{2+} channels. *Neuron*, 12: 1301–1318.

36 Ionescu, L., White, C., Cheung, K.-H., Shuai, J., Parker, I., Pearson, J. E., Foskett, J. K., and Mak, D.-O. D. (2007). Mode switching is the major mechanism of ligand regulation of $InsP_3$ receptor calcium release channels. *Journal of General Physiology*, 130(6): 631–645.

37 Keener, J. P. and Sneyd, J. (2009). *Mathematical Physiology I: Cellular physiology*, volume 8/1 of *Interdisciplinary Applied Mathematics*. New York: Springer, 2 edition.

38 Luvisetto, S., Fellin, T., Spagnolo, M., Hivert, B., Brust, P. F., Harpold, M. M., Stauderman, K. A., Williams, M. E., and Pietrobon, D. (2004). Modal gating of human $Ca_V2.1$ (P/Q-type) calcium channels: I. The slow and the fast gating modes and their modulation by subunits. *The Journal of General Physiology*, 124: 445–461.

39 Magleby, K. L. and Pallotta, B. S. (1983a). Burst kinetics of single calcium-activated potassium channels in cultured rat muscle. *Journal of Physiology-London*, 344: 605–623.

40 Magleby, K. L. and Pallotta, B. S. (1983b). Calcium dependence of open and shut interval distributions from calcium-activated potassium channels in cultured rat muscle. *Journal of Physiology-London*, 344: 585–604.

41 McManus, O. B. and Magleby, K. J. (1988). Kinetic states and modes of single large-conductance calcium-activated potassium channels in cultured rat skeletal-muscle. *Journal of Physiology-London*, 402: 79–120.

42 Metropolis, N., Rosenbluth, A. W., Rosenbluth, M. N., Teller, A. H., and Teller, E. (1953). Equation of state calculations by fast computing machines. *Journal of Chemical Physics*, 21(6): 1087–1092.

43 Milone, M., Wang, H.-L., Ohno, K., Prince, R., Fukudome, T., Shen, X.-M., Brengman, J. M., Griggs, R. C., Sine, S. M., and Engel, A. G. (1998). Mode switching kinetics produced by a naturally occurring mutation in the cytoplasmic loop of the human acetylcholine receptor ϵ subunit. *Neuron*, 20: 575–588.

44 Monod, J., Wyman, J., and Changeux, J. P. (1965). On the nature of allosteric transitions: A plausible model. *Journal of Molecular Biology*, 12: 88–118.

45 Naranjo, D. and Brehm, P. (1993). Modal shifts in acetylcholine receptor channel gating confer subunit-dependent desensitization. *Science*, 260: 1811–1814.

46 Neher, E. and Sakmann, B. (1976). Single-channel currents recorded from membrane of denervated frog muscle fibres. *Nature*, 260(5554): 799–802.

47 Popescu, G. and Auerbach, A. (2003). Modal gating of NMDA receptors and the shape of their synaptic response. *Nature Neuroscience*, 6(5): 476–483.

48 Popescu, G., Robert, A., Howe, J. R., and Auerbach, A. (2004). Reaction mechanism determines NMDA receptor response to repetitive stimulation. *Nature*, 430(7001): 790–793.

49 Qin, F., Auerbach, A., and Sachs, F. (1996). Idealization of single-channel currents using the segmental K-means method. *Biophysical Journal*, 70(2, Part 2): MP432.

50 Qin, F., Auerbach, A., and Sachs, F. (1997). Maximum likelihood estimation of aggregated Markov processes. *Proceedings of the Royal Society of London Series B-Biological Sciences*, 264: 375–383.

51 Raiffa, H. and Schlaifer, R. (1961). *Applied Statistical Decision Theory*. Boston, Massachusetts: Harvard University Graduate School of Business Administration.

52 Rosales, R. (2004). MCMC for Hidden Markov Models incorporating aggregation of states and filtering. *Bulletin of Mathematical Biology*, 66: 1173–1199.

53 Rosales, R., Stark, J. A., Fitzgerald, W. J., and Hladky, S. B. (2001). Bayesian Restoration of Ion Channel Records using Hidden Markov Models. *Biophysical Journal*, 80(3): 1088–1103.

54 Rosales, R. A., Fill, M., and Escobar, A. L. (2004). Calcium regulation of single ryanodine receptor channel gating analyzed using HMM/MCMC statistical methods. *The Journal of General Physiology*, 121: 533–553.

55 Rothberg, B. S., Bello, R. A., Song, L., and Magleby, K. L. (1996). High Ca^{2+} concentrations induce a low activity mode and reveal Ca^2+-independent long shut intervals in BK channels from rat muscle. *Journal of Physiology*, 493(3): 637–689.

56 Rothberg, B. S. and Magleby, K. L. (1998). Kinetic structure of Large-Conductance Ca^{2+}-activated K^+ channels suggests that the gating includes transitions through intermediate or secondary states—A mechanism for flickers. *Journal of General Physiology*, 111(6): 751–780.

57 Rothberg, B. S. and Magleby, K. L. (1999). Gating kinetics of single large-conductance Ca^{2+}-activated K^+ channels in high Ca^{2+} suggest a two-tiered allosteric gating mechanism. *Journal of General Physiology*, 114(1): 93–124.

58 Rothberg, B. S. and Magleby, K. L. (2000). Voltage and Ca^{2+} activation of single large-conductance Ca^{2+}-activated K^+ channels described by a two-tiered allosteric gating mechanism. *Journal of General Physiology*, 116: 75–99.

59 Siekmann, I., Crampin, E. J., and Sneyd, J. (2012a). MCMC can detect non-identifiable models. *Biophysical Journal*, 103(11): 1275–1286.

60 Siekmann, I., Wagner II, L. E., Yule, D., Crampin, E. J., and Sneyd, J. (2012b). A kinetic model of type I and type II IP_3R accounting for mode changes. *Biophysical Journal*, 103(4): 658–668.

61 Siekmann, I., Wagner II, L. E., Yule, D., Fox, C., Bryant, D., Crampin, E. J., and Sneyd, J. (2011). MCMC estimation of Markov models for ion channels. *Biophysical Journal*, 100: 1919–1929.

62 Singer-Lahat, D., Dascal, N., and Lotan, I. (1999). Modal behavior of the $k_v1.1$ channel conferred by the $k_v\beta1.1$ subunit and its regulation by dephosphorylation of $k_v1.1$. *Pflügers Archiv—European Journal of Physiology*, 439: 18–26.

63 Smith, A. F. M. (1975). A Bayesian approach to inference about a change-point in a sequence of random variables. *Biometrika*, 62(2): 407–416.

64 The, Y.-K. and Timmer, J. (2006). Analysis of single ion channel data incorporating time-interval omission and sampling. *Journal of the Royal Society Interface*, 3(6): 87–97.

65 Venkataramanan, L. and Sigworth, F. J. (2002). Applying hidden markov models to the analysis of single ion channel activity. *Biophysical Journal*, 82(4): 1930–1942.

66 Wagner, L. E. and Yule, D. I. (2012). Differential regulation of the $InsP_3$ receptor type-1 and -2 single channel properties by $InsP_3$, Ca^{2+} and ATP. *The Journal of Physiology*, 590(14): 3245–3259.

67 Yakubovich, D., Pastushenko, V., Bitler, A., Dessauer, C. W., and Dascal, N. (2000). Slow modal gating of single G protein-activated K^+ channels expressed in *xenopus* oocytes. *Journal of Physiology*, 524(3): 737–755.

68 Yue, D., Herzig, S., and Marban, E. (1990). Beta-adrenergic stimulation of calcium channels occurs by potentiation of high-activity gating modes. *Proceedings of the National Academy of Sciences of the USA*, 87: 753–757.

69 Zahradníková, A., Dura, M., and Györke, S. (1999). Modal gating transitions in cardiac ryanodine receptors during increases of Ca^{2+} concentration produced by photolysis of caged Ca^{2+}. *Pflügers Achiv—European Journal of Physiology*, 438: 283–288.

70 Zahradníková, A. and Zahradník, I. (1996). A minimal gating model for the cardiac calcium release channel. *Biophysical Journal*, 71: 2996–3012.